THE INSTITUTE FOR MOLECULAR ENGINEERING

Predicting complex materials properties: first principles calculations

Giulia Galli

University of Chicago
gagalli@uchicago.edu
http://galligroup.uchicago.edu/

ANL, QMC Training Program, July 17th, 2014

Fundamental science and materials design

Photovoltaics

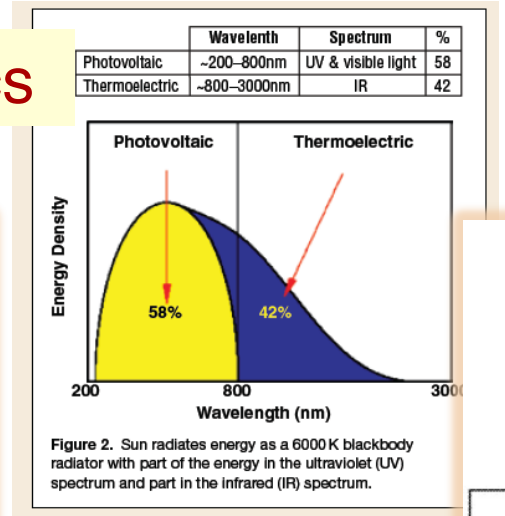

	Wavelenth	Spectrum	%
Photovoltaic	~200–800nm	UV & visible light	58
Thermoelectric	~800–3000nm	IR	42

Figure 2. Sun radiates energy as a 6000 K blackbody radiator with part of the energy in the ultraviolet (UV) spectrum and part in the infrared (IR) spectrum.

Solar to fuel

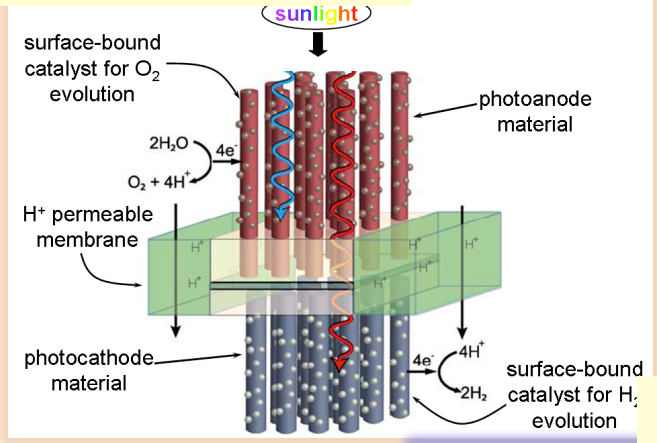

CCI Powering the planet:
http://www.ccisolar.caltech.edu/

Thermoelectrics

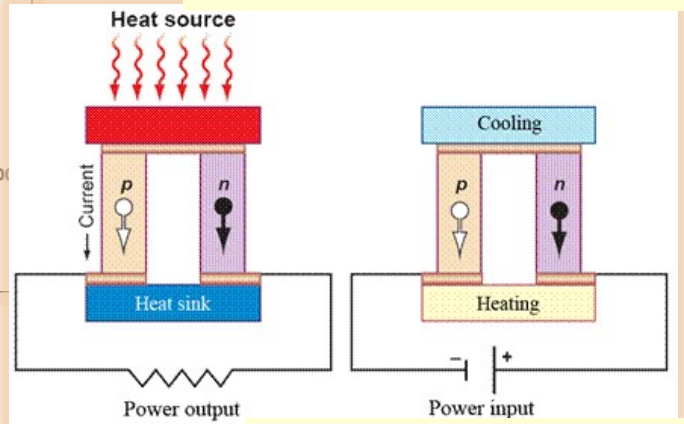

Carbon cycle

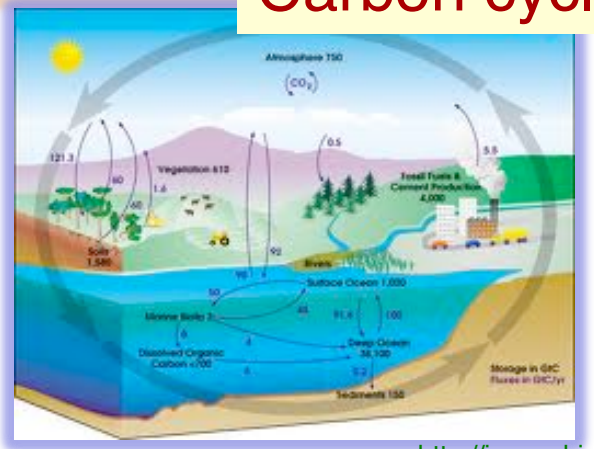

Deep Carbon Observatory:
http://deepcarbon.net/

Clean Water

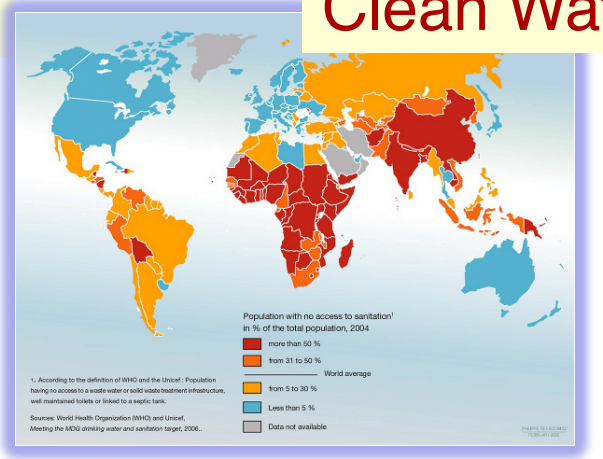

http://ime.uchicago.edu/features/the_global_challenge_access_to_clean_fresh_water/

Complex semiconductors and insulators for energy conversion processes

- Can nanostructuring semiconductors help to beat the Shockley-Queisser limit in solar energy conversion?

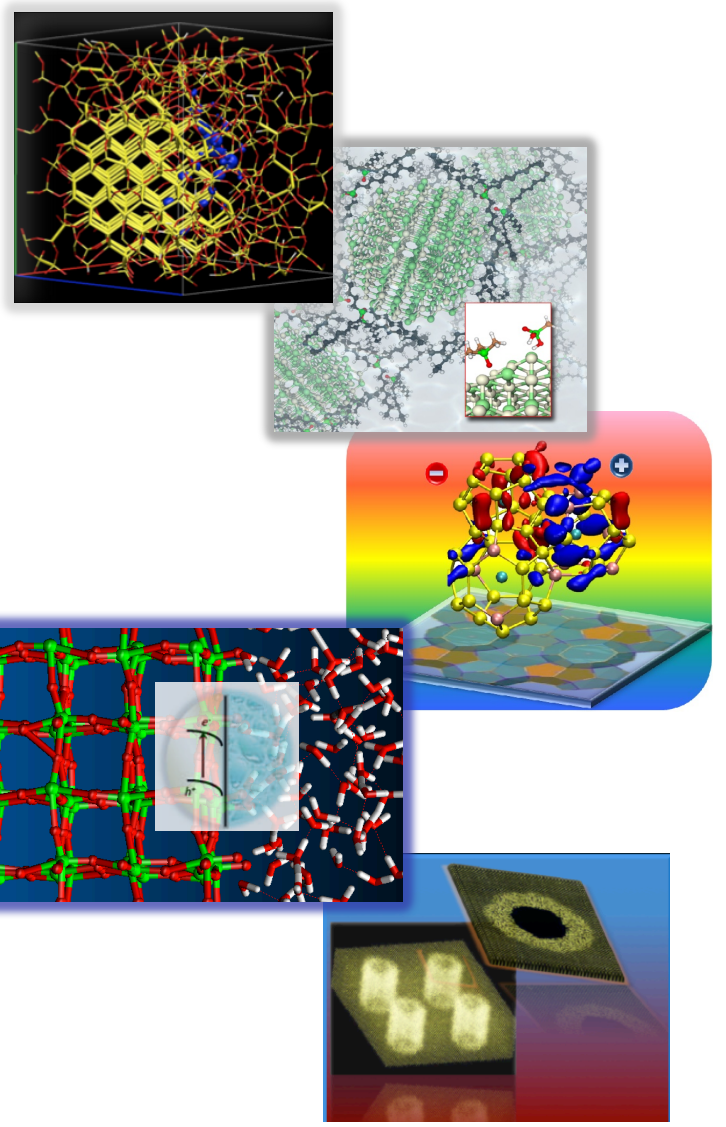

Materials & Fundamental physical phenomena/processes

- How do we engineer optical gaps & band edges in phoelectrodes for water oxidation?
- Are charge and phonon transport in nanostructured thermoelectrics fundamentally different than at the macroscopic scale?

Complex semiconductors for energy conversion processes

- Can nanostructuring semiconductors help to beat the Shockley-Queisser limit in solar energy conversion?
- How do we engineer optimal transport channels for electrons and holes in a photo-excited material?
- How do we engineer optical gaps & band edges in phoelectrodes for water oxidation?
- Are charge and phonon transport in nanostructured thermoelectrics fundamentally different than at the macroscopic scale?

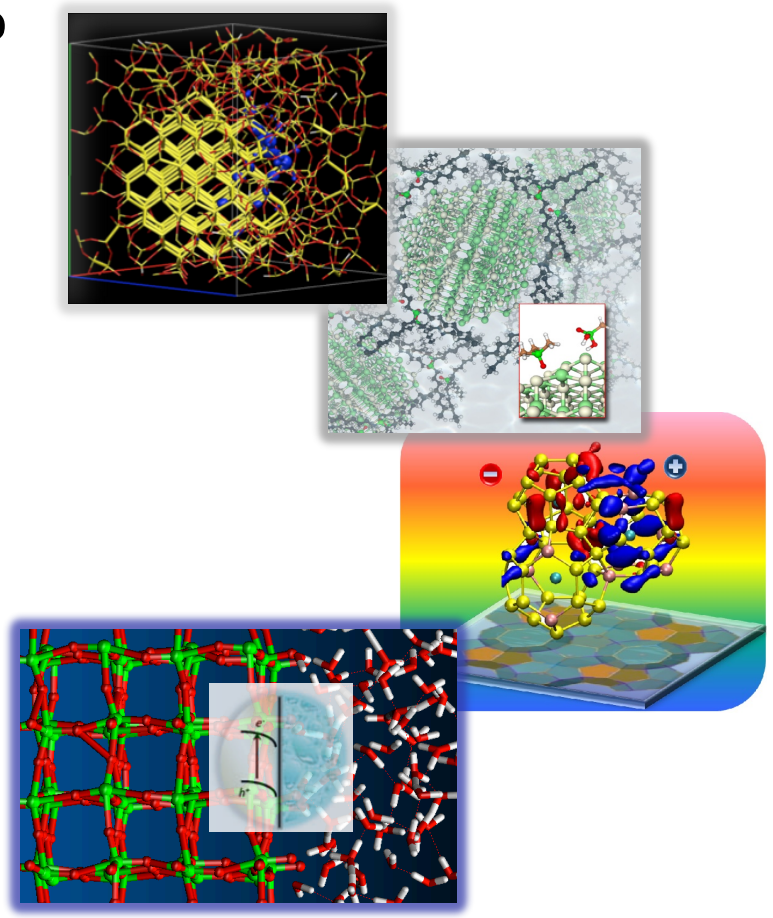

Excited states and transport properties

- Theoretical and computational strategies
- Short stories on solar energy conversion
  - —Embedded nanoparticles
  - —Si-based clathrates & perovskites
  - —Photo-electrodes for water catalysis

Theoretical and computational strategy

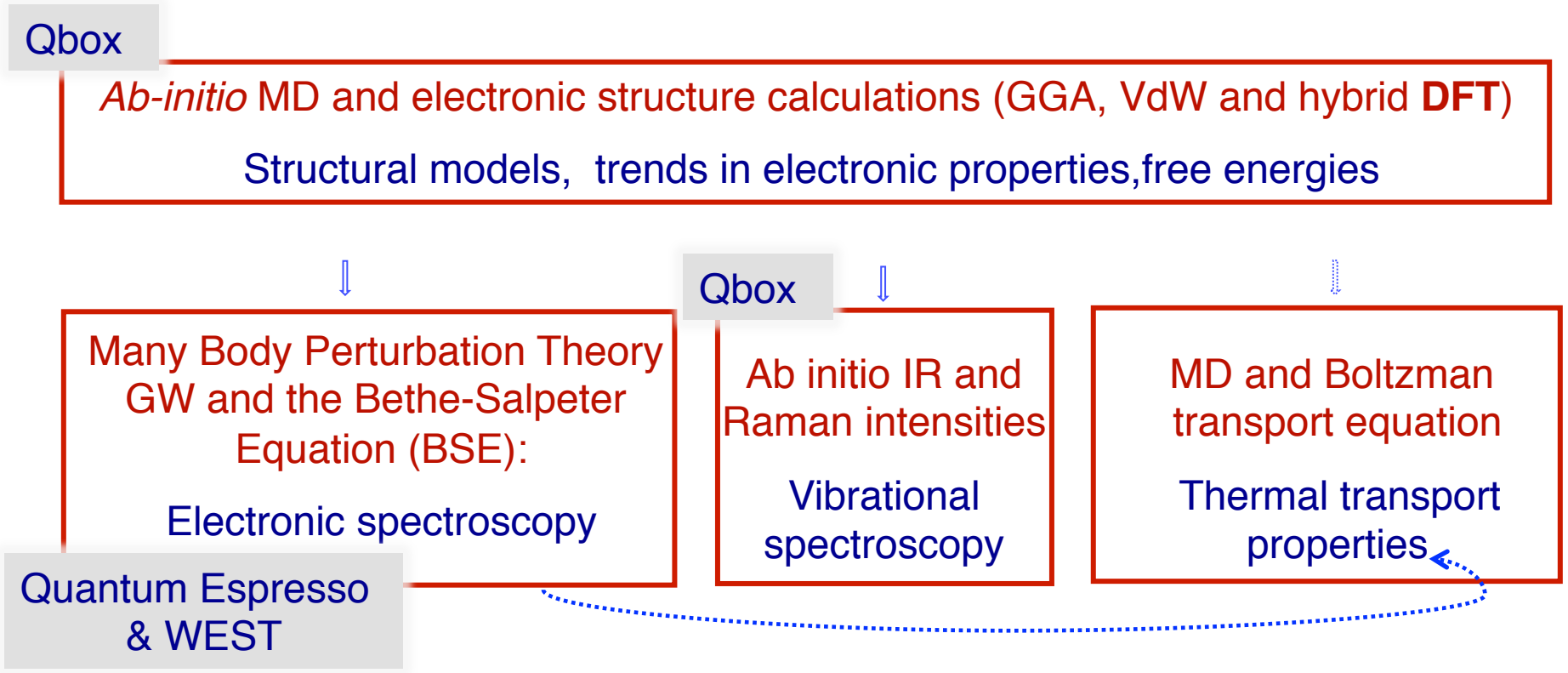

Y.Ping and D.Rocca and GG Chem. Soc. Rev. 2013

http://eslab.ucdavis.edu/software/qbox/

http://www.quantum-espresso.org/

Computational spectroscopy for realistic systems

New algorithmic developments together with optimized codes and modeling strategies are allowing us to address new problems in materials chemistry and physics

Computational spectroscopy for realistic systems

Ab-initio MD and electronic structure calculations (GGA, VdW and hybrid **DFT**)

Structural models, trends in electronic properties,free energies

⇩

Many Body Perturbation Theory GW and the Bethe-Salpeter Equation (BSE):

Electronic spectroscopy

⇩

Ab initio IR and Raman intensities

Vibrational spectroscopy

⇩

MD and Boltzman transport equation

Thermal transport properties

Y.Ping and D.Rocca and *GG* Chem. Soc. Rev. 2013

Photoemission Spectra: Quasi particle energies from MBPT (G_0W_0)

$$(T + V_{ext} + V_H)\psi_n(r) + \int dr' \Sigma(r, r', E_n)\psi_n(r') = E_n\psi_n(r)$$

$$\Sigma(r, r', i\omega) = \frac{1}{2\pi} \int d\omega' G(r, r', i(\omega - \omega'))W(r, r', i\omega')$$

- Self energy expressed in terms of eigenvalues and eigenvectors of the dielectric matrix
- Frequency integration using Lanczos algorithm and contour deformation

- **Algorithm enables GW calculations:**
  - without explicit calculation of empty single particle orbitals
  - without explicit diagonalization and storage of dielectric matrices
  - scaling: $N_{eig}\mathbf{N_{pw}}N_v^2$ (instead of $\mathbf{N_{pw}}^2N_vN_c$ where $N_c >> N_v$; $N_{pw} >> N_{eig}$)
  - numerical accuracy controlled by one single parameter

H. V. Nguyen, T.A. Pham, D.Rocca and GG Phys. Rev. B – Rapid Comm. 2012
T.A.Pham, H,V.Nguyen, D.Rocca and GG, Phys.Rev.B 2013

Optical spectra and multi-exciton generations

Optical spectra: absorption coeff. by solving the Bether Salpeter Equation (BSE):

- We solve the BSE by using the screened exact exchange self energy in the quantum Liouville equations (1st order perturbation theory)
- We compute the static dielectric screening iteratively, by using an eigenvalue decompositions ⟹ Full optical spectrum obtained with a numerical workload comparable to Hartree-Fock calculations

Multi-exciton generation: assume it mostly originates from impact ionization and compute conditional probabilities:

$$\Gamma_i = 2\pi \sum_f |\langle X_i | W | X X_f \rangle|^2 \delta(E_i - E_f)$$

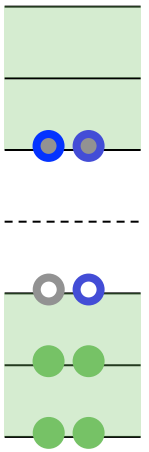

D. Rocca, D. Lu and G. Galli, *J. Chem. Phys.* **133**, 164109 (2010); D. Rocca, Y. Ping, R. Gebauer and G. Galli, *Phys. Rev. B*, **85**, 045116, (2012); Y. Ping, D. Rocca, G. Galli, *Chem. Soc. Rev.* **42**, 2437 (2013); M.Voros, A.Gali, D.Rocca,GG and G.Zimanyi PRB 2013

Computational spectroscopy for realistic systems

Optical spectra

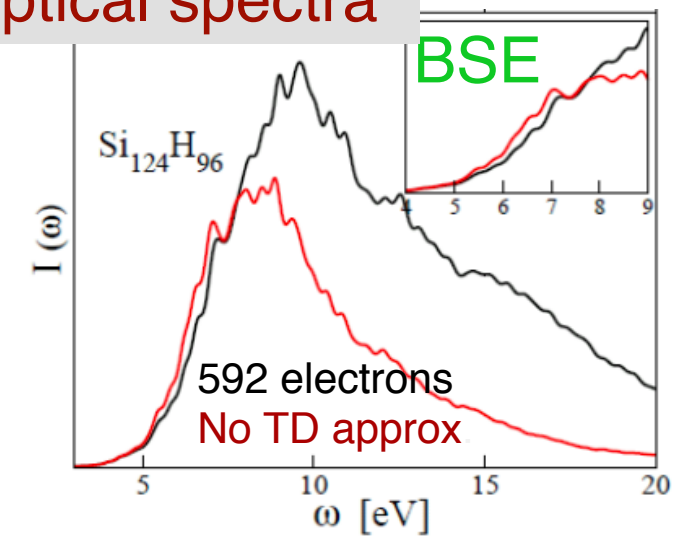

D.Rocca, M.Voros, A.Gali & GG, JCTC 2014

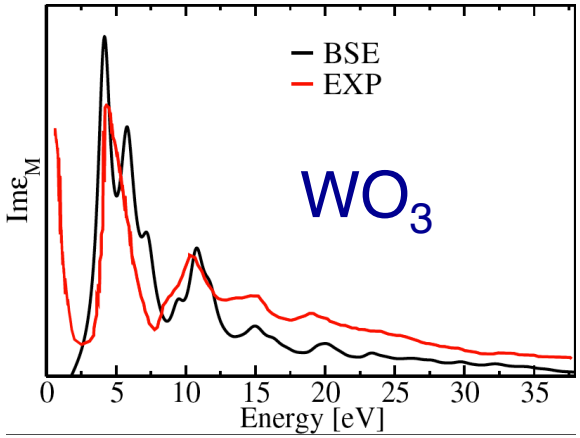

Y.Ping, D.Rocca, GG, PRB 2013

Photoemission and band offsets

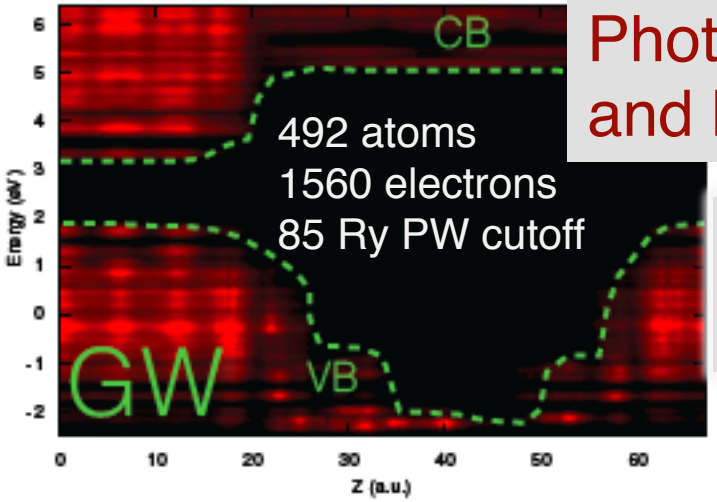

Qbox +
QE modules +
WEST-parallel

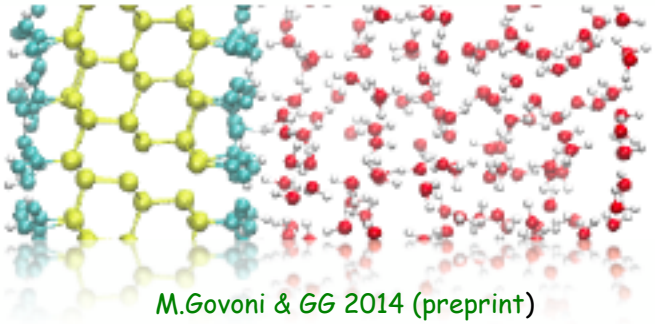

M.Govoni & GG 2014 (preprint)

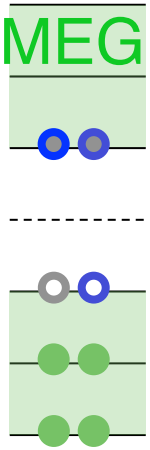

Multi-exciton generation

$$\Gamma_i = 2\pi \sum_f |\langle X_i | W | X X_f \rangle|^2 \delta(E_i - E_f)$$

M.Voros, A.Gali, D.Rocca,GG and G.Zimanyi PRB 2013

Computational spectroscopy for realistic systems

Ab-initio MD and electronic structure calculations (GGA, VdW and hybrid **DFT**)

Structural models, trends in electronic properties,free energies

⇩

Many Body Perturbation Theory GW and the Bethe-Salpeter Equation (BSE):

Electronic spectroscopy

⇩

Ab initio IR and Raman intensities

Vibrational spectroscopy

⇩

MD and Boltzman transport equation

Thermal transport properties

Y.Ping and D.Rocca and GG Chem. Soc. Rev. 2013

Fundamental understanding of interfacial electronic properties

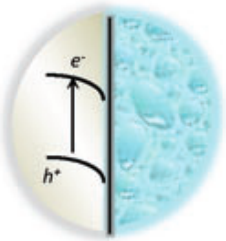

Light absorption by electrodes

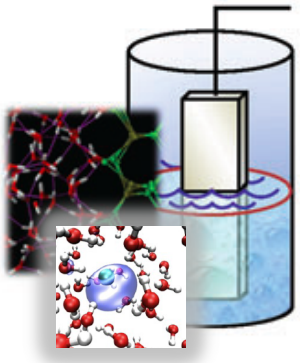

Band edge alignment between electrodes and water

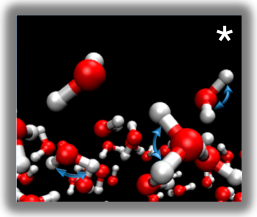

Characterization of water "species"at the interface

- Probe absorption processes and band edges of water and semiconductors and oxide with many body perturbation theory
- Probe interfaces and chemical reactions at interfaces with vibrational spectroscopy

*Y.Nagata et al. JPC-Lett 2013

Raman spectra obtained from coupled ab initio MD and Density Fcnt. Pert. Theory calculations

- Intensity of Raman spectra from time correlation functions of the polarizability tensor

$$I_{iso}^{Raman} \propto \int dt e^{-i\omega t} \left\langle \bar{\alpha}(0)\bar{\alpha}(t) \right\rangle \qquad I_{aniso}^{Raman} \propto \int dt e^{-i\omega t} \left\langle \frac{2}{15} \mathrm{Tr}\left(\boldsymbol{\beta}(0)\boldsymbol{\beta}(t)\right) \right\rangle$$

$$\boldsymbol{\alpha} = \bar{\alpha} I + \boldsymbol{\beta} \qquad \bar{\alpha} = \mathrm{Tr}(\boldsymbol{\alpha})/3$$

- Polarizability tensor computed within density functional perturbation theory (DFPT)* on ab-initio MD trajectories **

$$(H_{SCF} - \varepsilon_n)\left|\bar{\psi}_n^{\mu}\right\rangle = -P_c\left[H_{SCF}, \mathbf{r}_{\mu}\right]\left|\psi_n\right\rangle \qquad (H_{SCF} - \varepsilon_n)\left|\Delta^{\mathrm{E}}\psi_n\right\rangle = -e\sum_{\mu}\mathrm{E}^{\mu}\left|\bar{\psi}_n^{\mu}\right\rangle - P_c\Delta V^{lf}\left|\psi_n\right\rangle$$

$$\mathrm{P}^{\mu} = -\frac{4e}{V}\sum_{n=1}^{N}\left\langle \bar{\psi}_n^{\mu}\middle|\Delta^{\mathrm{E}}\psi_n\right\rangle \qquad \alpha^{\mu\nu} = \mathrm{P}^{\mu}/\mathrm{E}^{\nu}$$

*S. Baroni *et al.* Rev. Mod. Phys. 2001, 73, 515; ** Q.Wan, L.Spanu, G.Galli and F.Gygi, JCTC 2013

Raman spectra obtained from coupled ab initio MD and Density Fcnt. Pert. Theory calculations

- Intensity of Raman spectra from time correlation functions of the polarizability tensor

$$I_{iso}^{Raman} \propto \int dt e^{-i\omega t} \langle \bar{\alpha}(0)\bar{\alpha}(t) \rangle \quad I_{aniso}^{Raman} \propto \int dt e^{-i\omega t} \left\langle \frac{2}{15} \mathrm{Tr}\left(\beta(0)\beta(t)\right) \right\rangle$$

$$\alpha = \bar{\alpha} I + \beta \quad \bar{\alpha} = \mathrm{Tr}(\alpha)/3$$

- Intensity of IR spectra from time correlation functions of molecular dipole

$$\alpha(\omega) = \frac{2\pi\omega^2\beta}{3cVn(\omega)} \int_{-\infty}^{\infty} dt\, e^{-i\omega t} \langle \sum_{ij} \mu_i(0) \cdot \mu_j(t) \rangle$$

- Sum frequency generation spectra from dipole-polarizability correlations

$$\chi_{ijk}(\omega) \propto \int dt\, e^{i\omega t} \langle \alpha_{ij}(0) \mu_k(t) \rangle$$

*S. Baroni *et al.* Rev. Mod. Phys. 2001, 73, 515; ** Q.Wan, L.Spanu, G.Galli and F.Gygi, JCTC 2013

Computational spectroscopy for realistic systems

New algorithmic developments together with optimized codes and modeling strategies are allowing us to address new problems in materials chemistry and physics

Computational spectroscopy for realistic systems

Accuracy of calculations still heavily impacted by underlying DFT description of single particle states

Excited states and transport properties

- Theoretical and computational strategies

- Short stories on solar energy conversion
  - —Embedded nanoparticles
  - —Si-based clathrates
  - —Photo-electrodes for water catalysis

Semiconducting nanostructures for 3rd generation photovoltaics (PV)

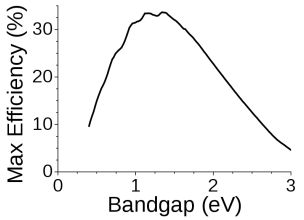

- Beyond the Shockley-Queisser limit (33.7% ; ideal p-n junction with 1.34 eV band gap) with a single band gap solar cell
- Avoid converting light into heat → Multi-exciton generation (MEG)
  - Quantum confinement "helps" MEG but in "friendly" materials pushes electronic gap beyond solar spectrum
  - Charge extraction and transport in nanostructures: difficult to engineer and control

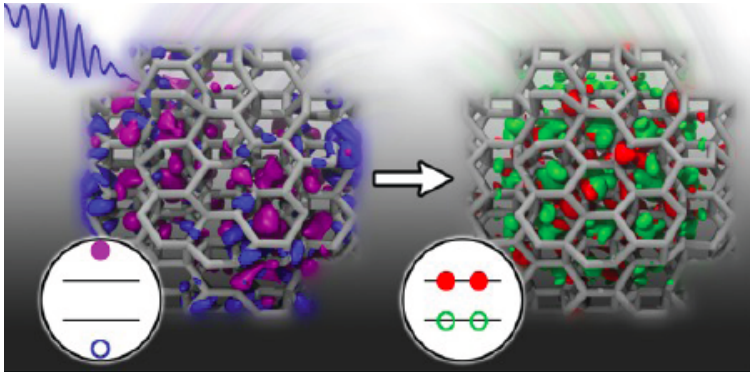

Semiconducting nanostructures for 3rd generation photovoltaics (PV)

- Beyond the Shockley-Queisser limit (33.7% ; ideal p-n junction with 1.34 eV band gap) with a single band gap solar cell

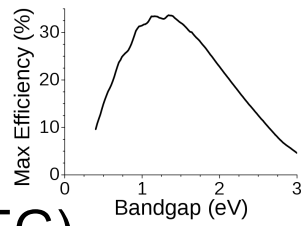

- Avoid converting light into heat → Multi-exciton generation (MEG)

Problem: Design realistic models of semiconductor nanostructures exhibiting efficient MEGs *and* favorable charge extraction and transport mechanisms

- Compute MEG rates from first principles
- Devise models of embedded NPs
- Understand charge transport

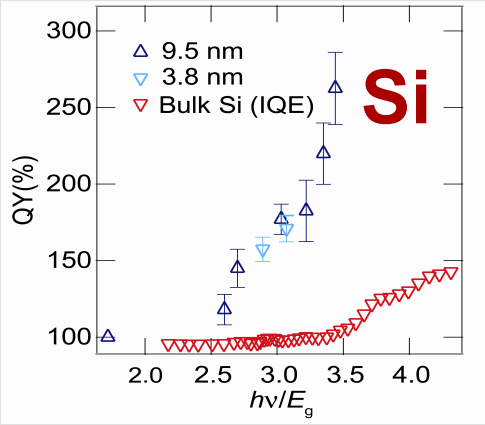

A.Nozik et al. Nanolett. 2007

Find Si NPs with 'solar' gaps & efficient MEGs

`High pressure Si cores` → lower the gap and increase multi-exciton generation probability

$$E_n^{qp} = \varepsilon_n + \langle\psi_n|\hat{\Sigma}(E_n^{qp})|\psi_n\rangle - \langle\psi_n|\hat{V}_{xc}|\psi_n\rangle$$

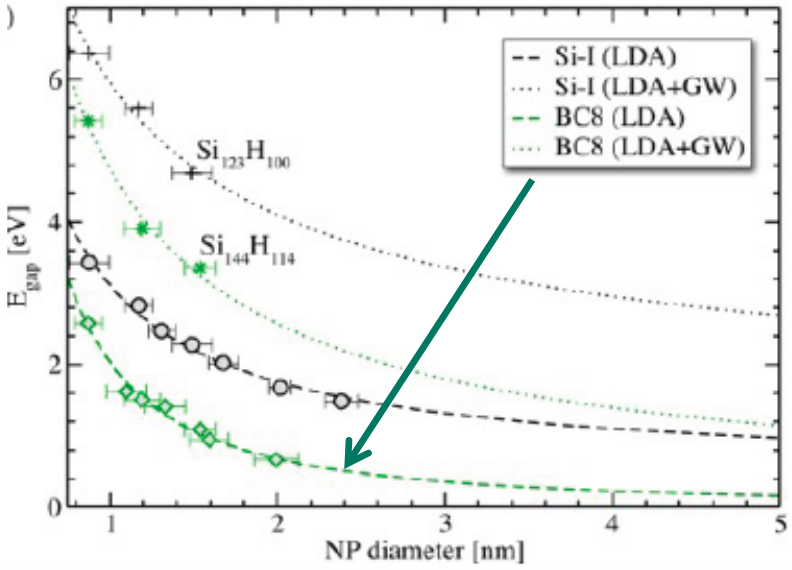

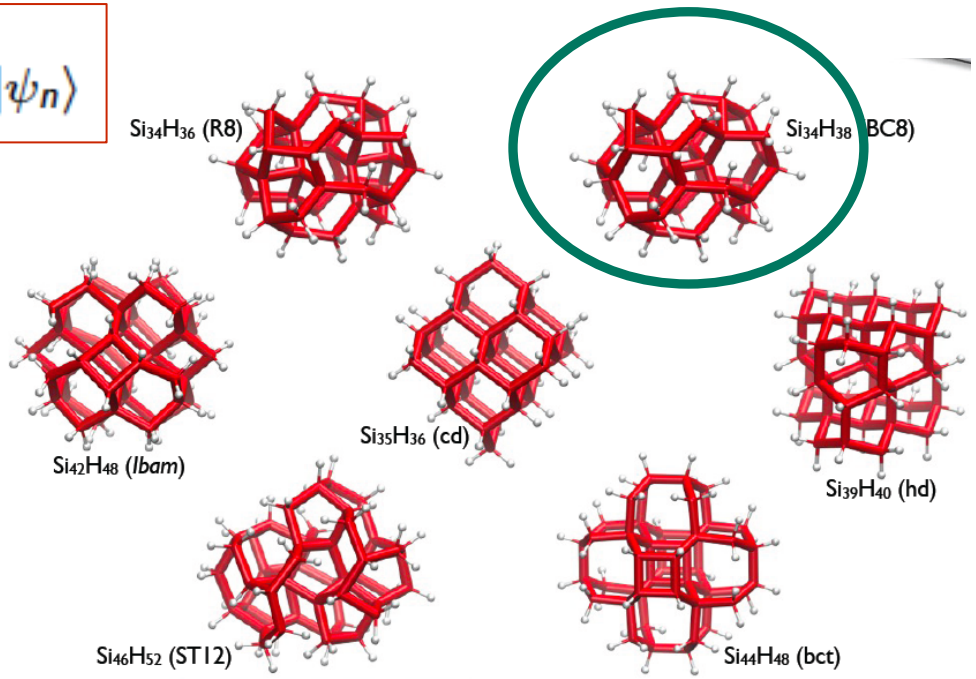

M.Voros, A.Gali, D.Rocca,GG and G.Zimanyi, PRB 2013; S.Wipperman, M.Voros, A.Gali, G.Zymanyi and GG Phys. Rev. Lett. 2013

Find Si NPs with ‘solar’ gaps & efficient MEGs

`High pressure Si cores` → lower the gap and increase multi-exciton generation probability

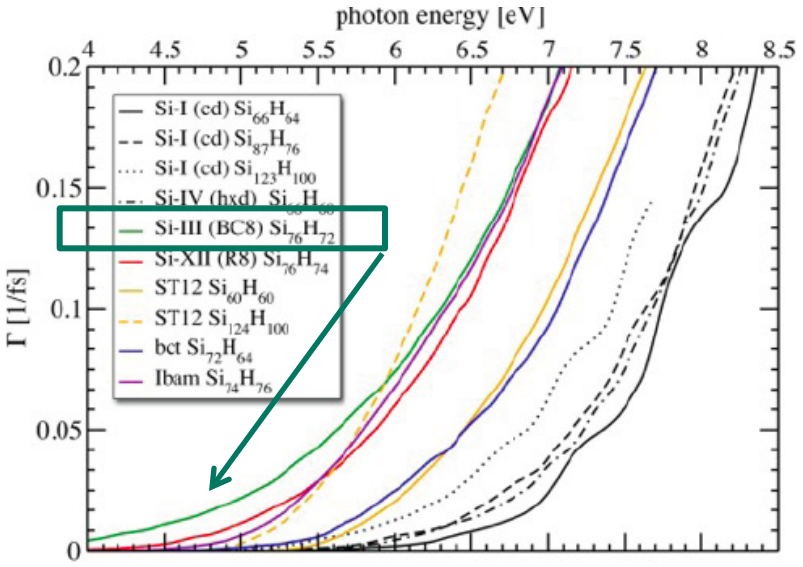

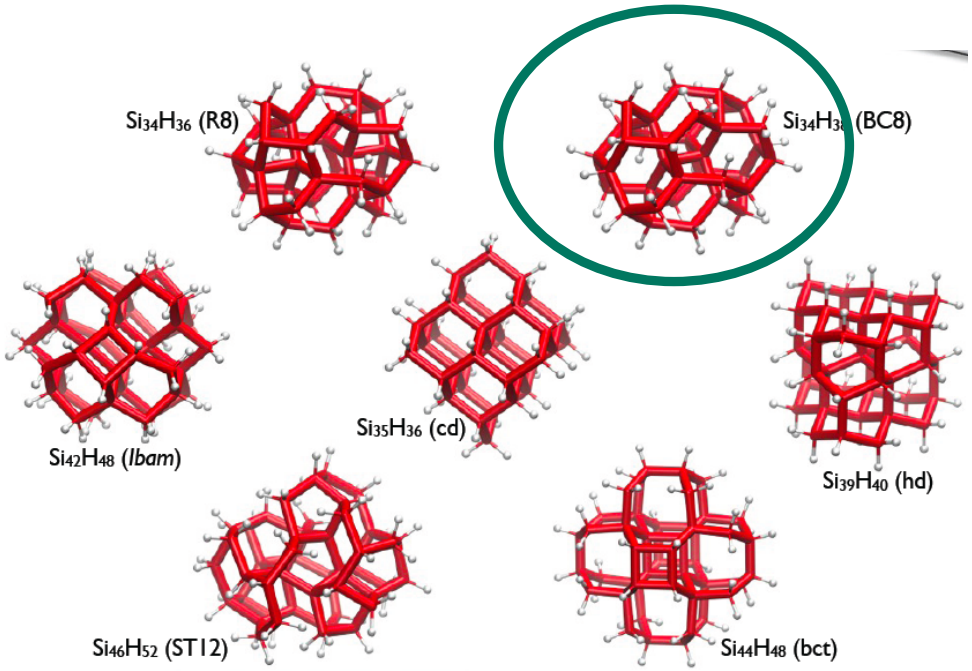

=> BC8 NPs allow for the first time for efficient MEG within the solar spectrum!

M.Voros, A.Gali, D.Rocca,GG and G.Zimanyi Phys. Rev. B 2013; S.Wipperman, M.Voros, A.Gali, G.Zymanyi and GG Phys. Rev. Lett. 2013

BC8 nanoparticles discovered in black Si and synthetized via colloidal route

- Laser induced recoil pressure waves create BC8&R8 Si nanoparticles in a-Si regions within core of nanopillars

M. Smith, E. Mazur *et al.*, J. Appl. Phys. **110**, 053524 (2011)

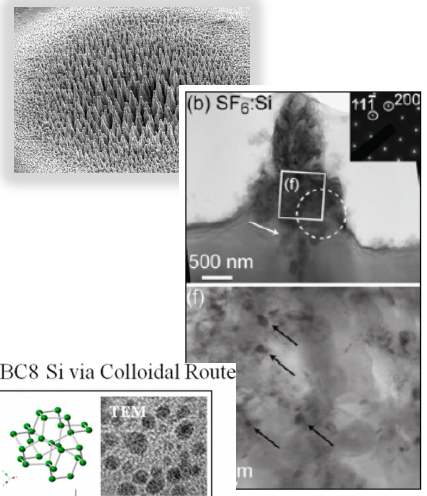

- Colloidal route (reduction of SiI_4 with n-butyllithium, capped with octanol and precipitated from solution)

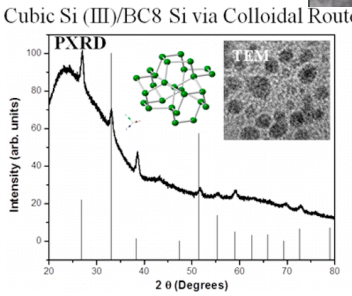

Garguly et al., JACS 2014

NPs embedded in solid matrices

Si-I in a-Si

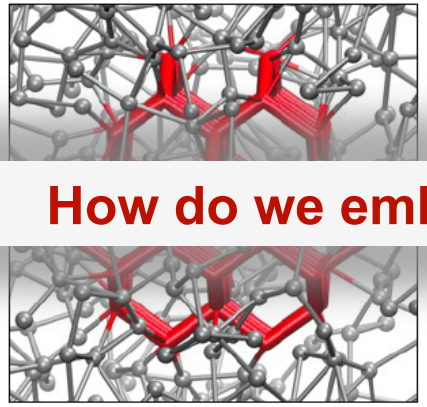

Si-III (BC8) in a-Si

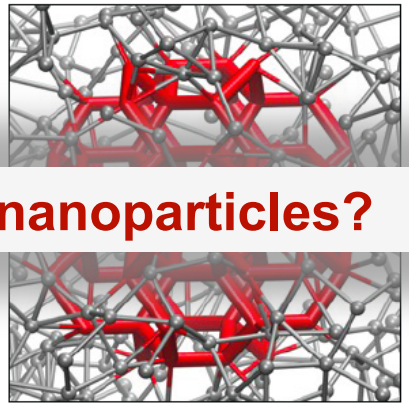

How do we embed nanoparticles?

T.S.Li, F.Gygi and GG, Phys Rev Lett 2011

Joint computational synthesis and characterization from ab initio MD

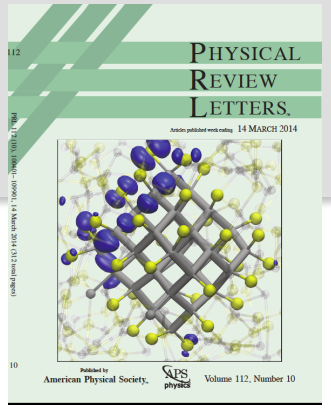

- Ab initio MD: Insert Si nanoparticle in crystalline ZnS; amorphize ZnS matrix, remove small Zn clusters
  - S is drawn from the matrix and the Si surface is terminated by sulfur
  - The electronic gap of the NP is substantially lowered
- Engineer S content to form type-II heterojunction

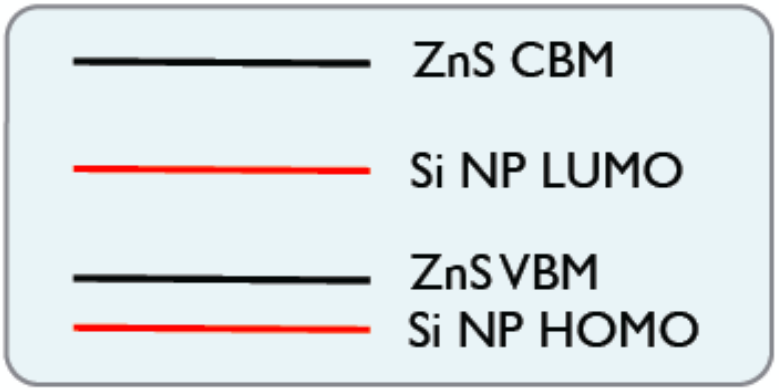

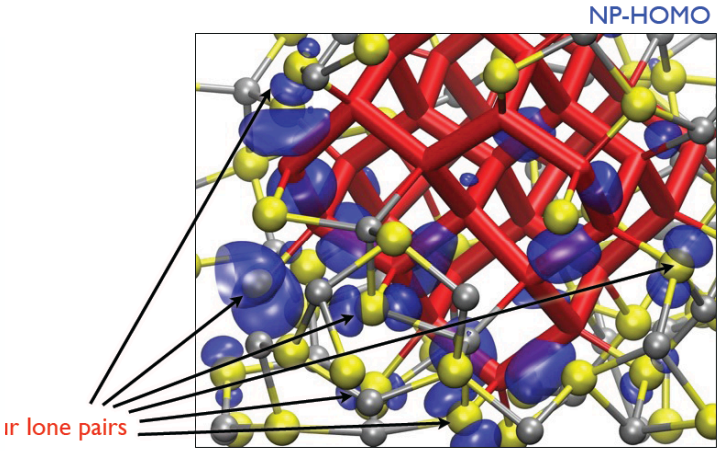

S.Wipperman, M.Voros, A.Gali, F.Gygi and G.Zymanyi and GG Phys Rev Lett 2014

Joint computational synthesis and characterization

- Computational spectroscopy:
  - Verify band offsets and band gaps found @PBE level of theory with hybrid functionals * and GW calculations **
  - Analyze localization properties of valence and conduction states and relate them to recombination rates
  - *Surgery to extract NP with relevant shell to compute MEG*

Solar nanocomposites with complementary charge extraction pathways for electrons and holes: Si embedded in ZnS

S.Wipperman, M.Voros, A.Gali, F.Gygi, G. Zymanyi and GG PRL 2014

Naturally nanostructured Si

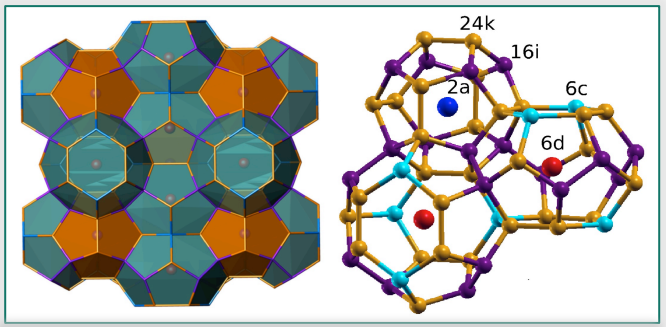

Si based clathrates: $K_8Al_8Si_{38}$

Y.He and GG 2013 Nanolett. 2014

Newly synthesized type I clathrate with low thermal conductivity, good thermal stability and promising thermoelectric properties

Can it be a good solar material as well?

Y.He, F.Sui, S.Kauzlarich and GG, EES-Comm 2014

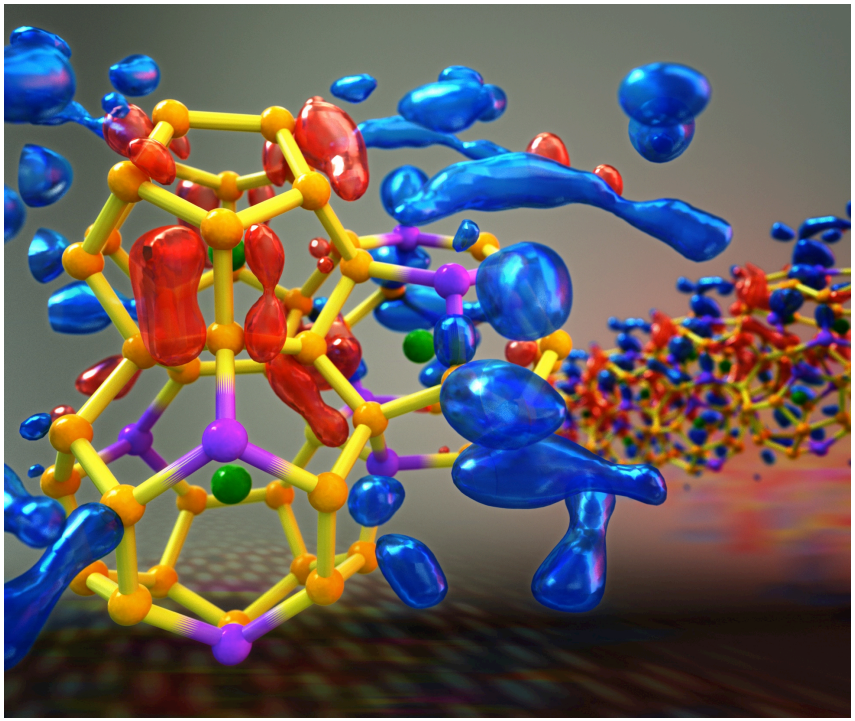

Naturally nanostructured Si

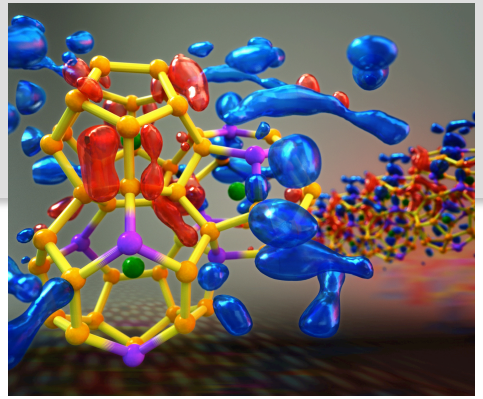

Our predictions:

- Quasi direct band gap of ~ 1 eV, tunable in the IR and visible range by strain engineering
- Mobilities much superior to a-Si and 6 to 10 smaller than c-Si
- Holes and electrons localized on different cages

Experiments:

Computed electron mobility: ~49 $cm^2/V/s$ at room temperature;

Measured electron mobility by Hall effect : ~39 $cm^2/V/s$

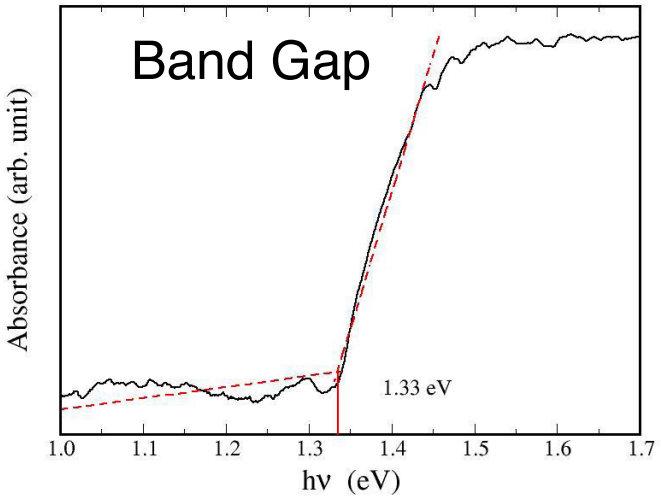

$K_8Al_8Si_{38}$ is a promising photovoltaic material

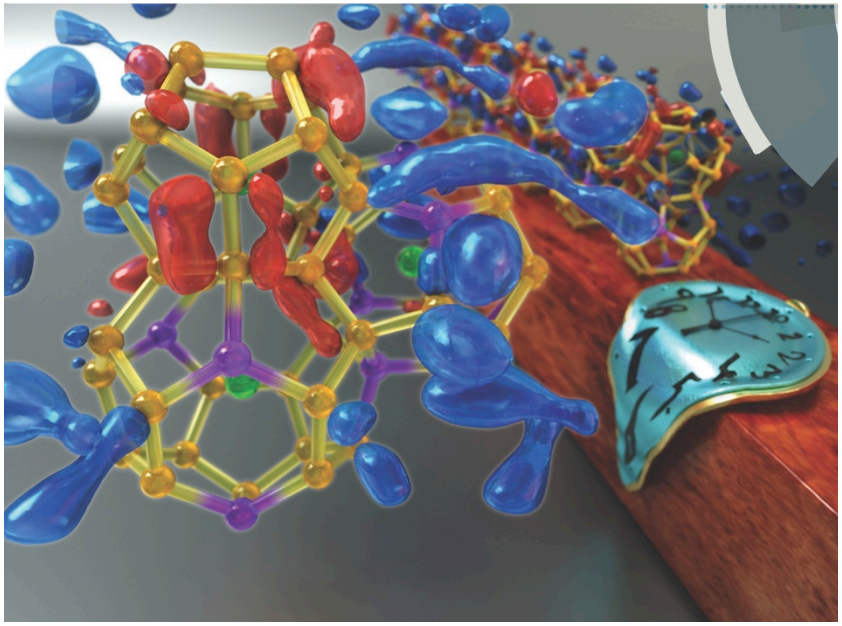

- Small thermal conductivity: ~1.8 W/mK
- Stable over a wide temperature range : up to 1050 K
- Cheap, Earth abundant elements
- Direct band gap: 0.5~1.4 eV
- Low carrier recombination rate
- High carrier mobilities

Y.He, F.Sui, S.Kauzlarich and GG, EES-Comm 2014

Y.He and GG Nanolett. 2014

Excited states and transport properties

- Theoretical and computational strategies

- Short stories on solar energy conversion
  - —Embedded nanoparticles
  - —Si-based clathrates
  - —Photo-electrodes for water catalysis

Search for “good” materials for photoanode and photocathode for water splitting

$$H_2O \rightarrow \tfrac{1}{2}O_2(\Delta) + H_2(g); \quad \Delta G = +237\ \text{kJ/mol}$$

$$(1.3\ \text{eV/e}, \lambda\text{min} = 1100\ \text{nm})$$

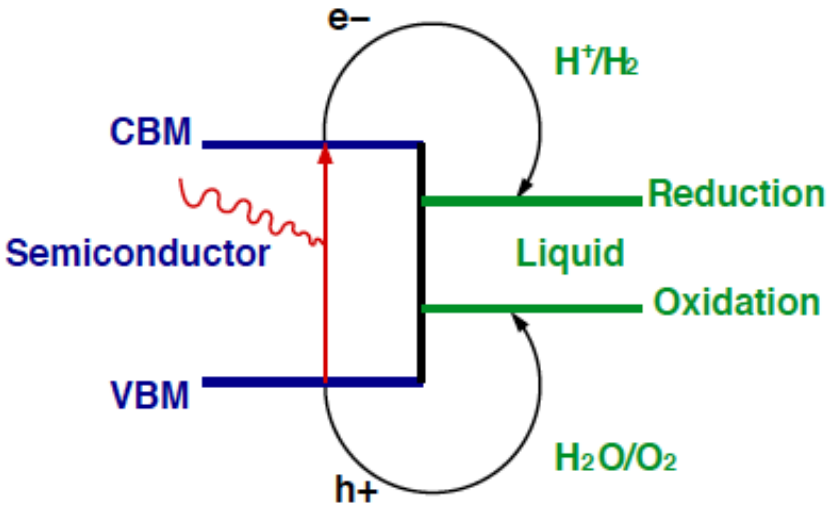

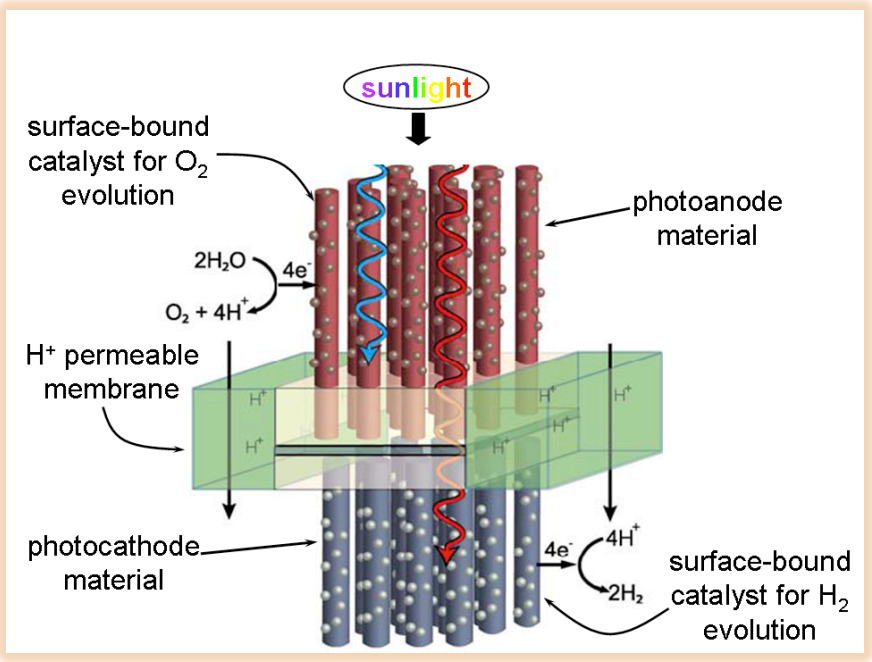

Ionization potential and electron affinity of liquid water

- Liquid water: samples of 512 electrons, generated by "*ab-initio*" simulations

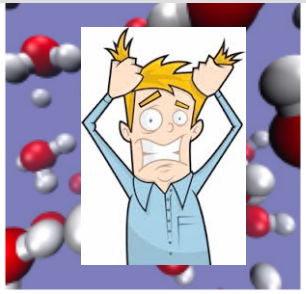

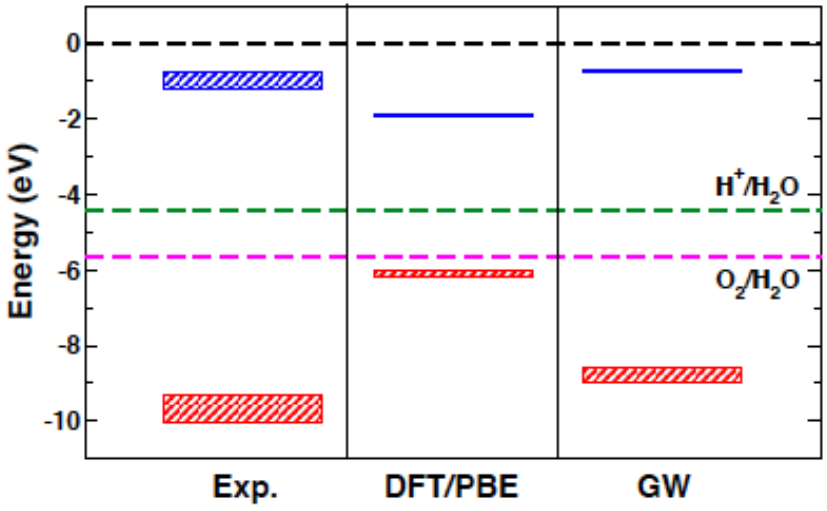

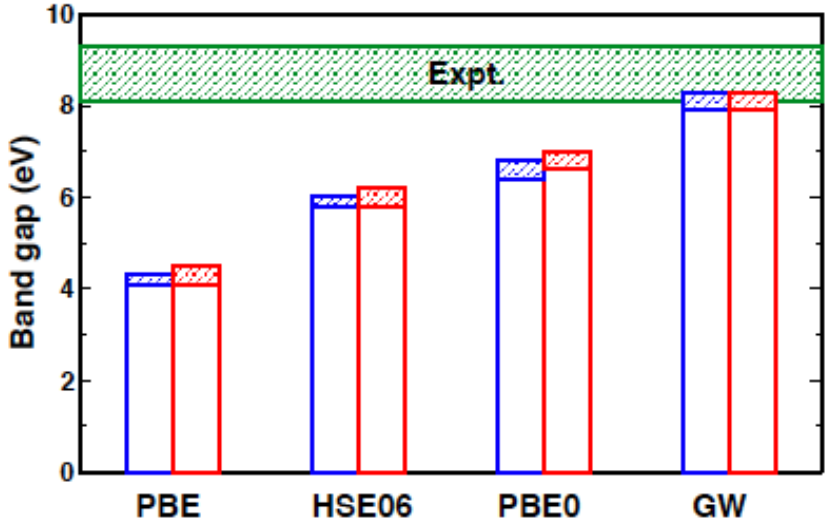

- Beyond DFT: We showed that GW corrections are crucial to obtain band edge positions in good agreement with experiments

T.A.Pham, C.Zhang, E.Schwegler and GG, Phys.Rev.B-RC (2014)

Band-edges of functionalized Si surfaces in water

Ab initio MD + band offsets calculations @ G_0W_0 level

- Solid-liquid interaction is not negligible even in the case of hydrophobic surfaces

T.A.Pham, D. Lee, E.Schwegler and GG. 2014 (preprint)

Hydrophilic surface: multiple effects involved in VBM and CBM shifts

- Water orientation
- Charge transfer

Search for “good” materials for photoanode and photocathode for water splitting

Doped-WO_3 and solid solutions

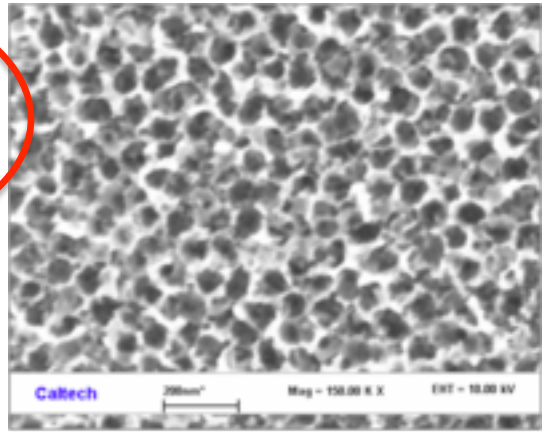

- How can we modify the material’s structure and/or morphology so as to decrease its band gap (~ 2.6 eV) and approach its valence band to the redox of water?

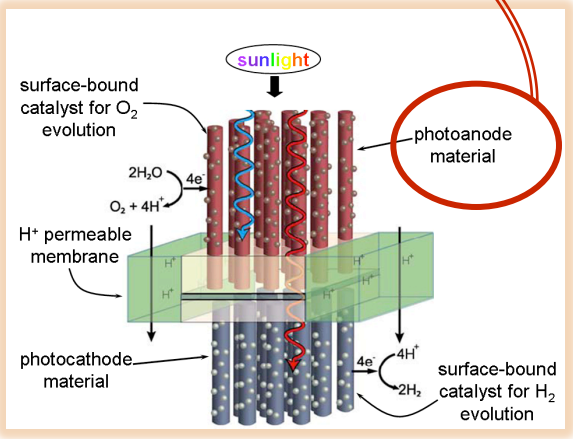

Band edge engineering

Optimize the band edge position of WO_3 :

- Different phases of solid WO_3
- Intercalation of small molecules (N_2) in WO_3 lattice
- Solid solutions

Screening materials: Generalized Kohn-Sham Formalism

- Non-local potential

$$v^{\mathrm{GKS}}(\mathbf{r},\mathbf{r}') = v_H(\mathbf{r}) + v_{xc}(\mathbf{r},\mathbf{r}') + v_{ext}(\mathbf{r})$$

- Full & range separated hybrids (RSH)

$$v_{xc}(\mathbf{r},\mathbf{r}') = \beta v_{exx}^{\mathrm{SR}}(\mathbf{r},\mathbf{r}') + \alpha v_{exx}^{\mathrm{LR}}(\mathbf{r},\mathbf{r}') + (1-\beta)v_x^{\mathrm{SR}}(\mathbf{r}) + (1-\alpha)v_x^{\mathrm{LR}}(\mathbf{r}) + v_c(\mathbf{r})$$

for example: $$v_{exx}^{\mathrm{LR}}(\mathbf{r},\mathbf{r}') = -\sum_{i=1}^{\mathrm{N_{occ}}} \phi_i(\mathbf{r})\phi_i^*(\mathbf{r}')\frac{\mathrm{erf}(\omega|\mathbf{r}-\mathbf{r}'|)}{|\mathbf{r}-\mathbf{r}'|}$$

Functional Name	Type of RSH	α	β	ω
PBE	none	0	0	0
PBE0	full	0.25	0	∞
HSE06	short	0	0.25	0.11
ω-LC-PBE	long	1.0	0	0.4

Focus on full-range hybrid $\beta = 0$, $\omega = \infty$ with one mixing parameter α

Self-Consistent Hybrid (sc-hybrid)

- A parameter free hybrid density functional for periodic systems
- The fraction of Hartree-Fock exchange (α) is determined self-consistently.

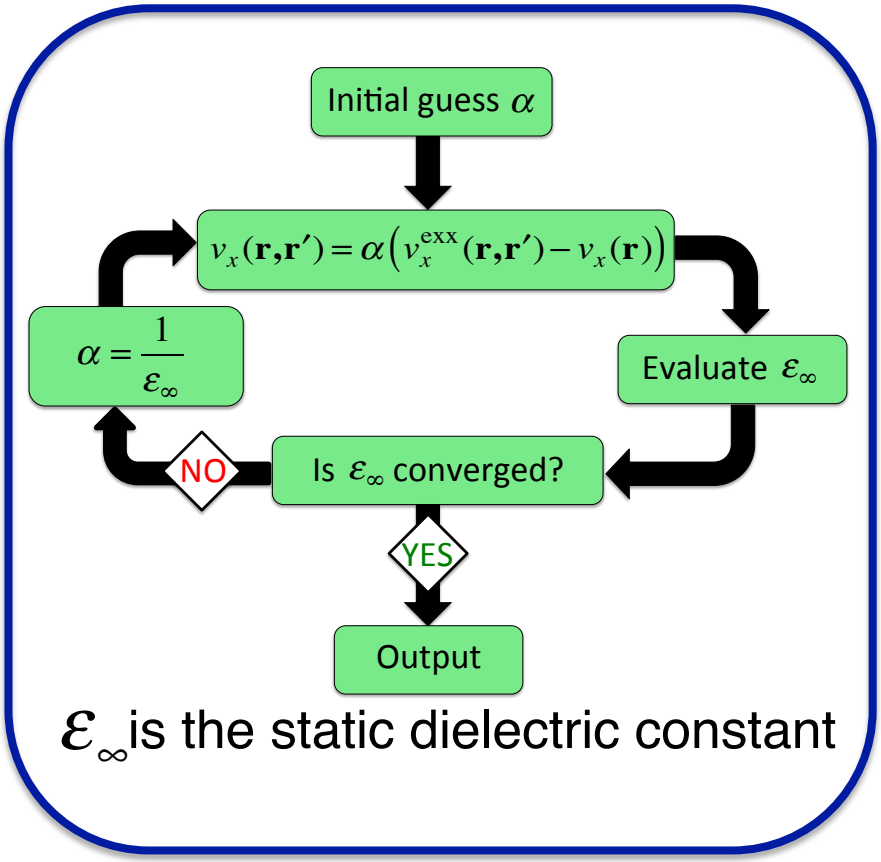

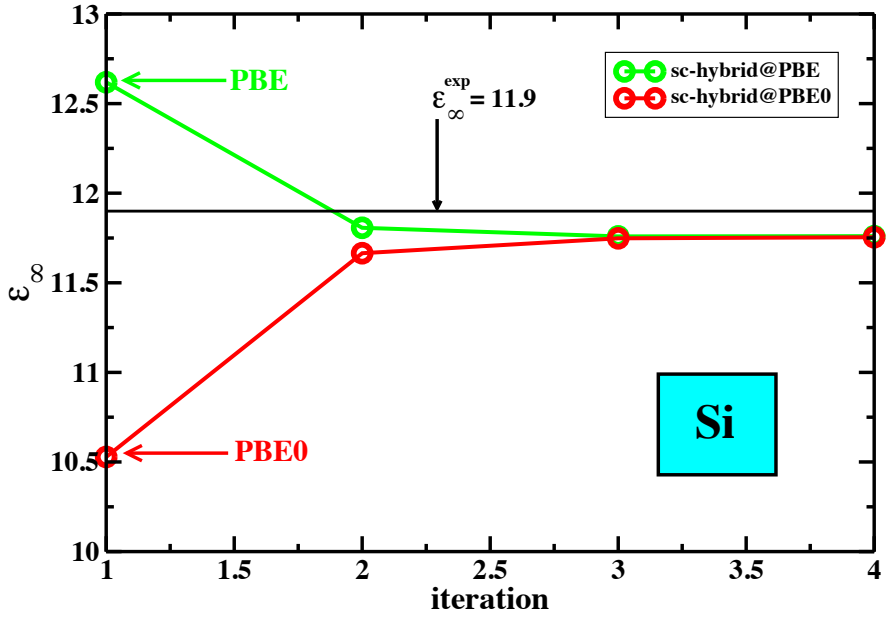

- No empirical input
- Cost: same order of magnitude as an ordinary hybrid calculation
- Applicable to all condensed phases

J.Skone, M.Govoni and GG, Phys. Rev. B 2014

Self-Consistent Hybrids (sc-hybrid)

- A wide array of semiconductors and insulators

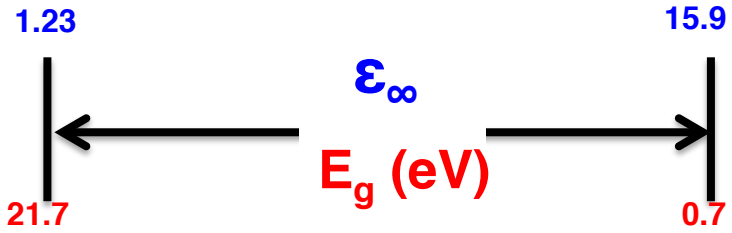

- CRYSTAL09[a] electronic structure package
- All-electron calc. except W and Hf (ECPs)
- Basis sets modified from Alhrich's def2-TZVPP and def2-QZVPP molecular basis
- Polarizabilites evaluated with CPKS[b] implementation in CRYSTAL09

[a] Dovesi, et al. *Zeitschrift für Kristallographie.* **220**, 571 (2005).
[b] Rérart, et al. *J. of Phys.: Conf. Series.* **117**, 012016 (2008).

Comparison with experiment: dielectric constant

$$\epsilon_{ij} = \delta_{ij} + \frac{4\pi e^2}{V}\chi_{ij}$$

polarizability χ_{ij} volume V

Mean Absolute Errors

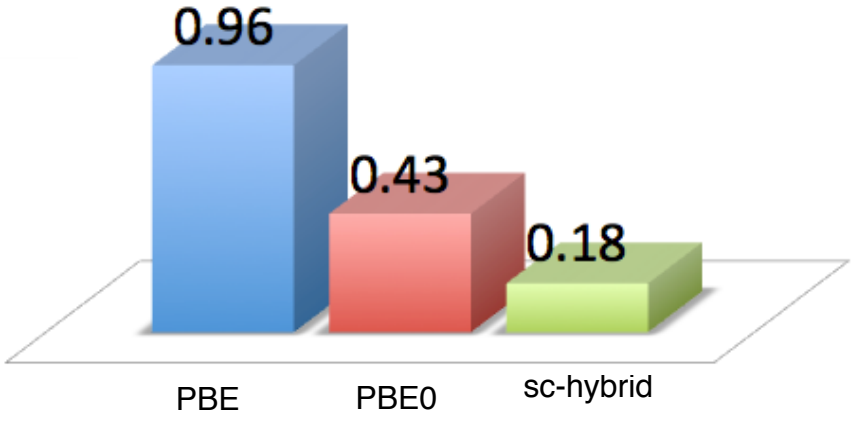

- sc-hybrid results in excellent agreement with experimental macroscopic dielectric constants

	PBE $\alpha = 0$	PBE0 $\alpha = 0.25$	sc-hybrid $\alpha = 1/\text{sc-}\epsilon_\infty$	Exp.
Ge	–	12.77	15.65	15.9
Si	12.62	10.53	11.76	11.9
AlP	7.82	6.85	7.23	7.54
SiC	6.94	6.28	6.50	6.52
TiO_2	7.91	5.96	6.56	6.34
NiO	16.98	4.74	5.49	5.76
C	5.83	5.54	5.61	5.70
CoO	–	4.52	4.92	5.35
GaN	5.78	5.0	5.14	5.30
ZnS	5.58	4.8	4.95	5.13
MnO	7.62	4.32	4.45	4.95
WO_3	5.46	4.60	4.72	4.81
BN	4.59	4.37	4.40	4.50
HfO_2	4.54	3.9	3.97	4.41
AlN	4.54	4.15	4.16	4.18
ZnO	4.66	3.54	3.46	3.74
Al_2O_3	3.27	3.07	3.01	3.10
MgO	3.12	2.89	2.81	2.96
LiCl	2.96	2.82	2.77	2.70
NaCl	2.49	2.37	2.29	2.40
LiF	1.97	1.87	1.77	1.90
H_2O	1.80	1.73	1.65	1.72
Ar	1.74	1.70	1.66	1.66
Ne	1.28	1.24	1.21	1.23
ME	0.96	-0.41	-0.15	–
MAE	0.96	0.43	0.18	–
MRE (%)	18.5	-5.1	-3.1	–
MARE (%)	18.5	6.2	4.0	–

Comparison with experiment: electronic gaps

	Type	PBE $\alpha = 0$	PBE0 $\alpha = 0.25$	hybrid $\alpha = 1/\epsilon_\infty^{PBE}$	hybrid $\alpha = 1/\epsilon_\infty^{PBE0}$	sc-hybrid $\alpha = 1/\text{sc-}\epsilon_\infty$	Exp.
Ge	(dC)	0.00	1.53	–	0.77	0.71	0.74 [85]
Si	(dC)	0.62	1.75	0.96	1.03	0.99	1.17 [85]
AlP	(ZB)	1.64	2.98	2.31	2.41	2.37	2.51 [86]
SiC	(ZB)	1.37	2.91	2.23	2.33	2.29	2.39 [87]
TiO_2	(Ru)	1.81	3.92	2.83	3.18	3.05	3.3 [88]
NiO	(RS)	0.97	5.28	2.00	4.61	4.11	4.3 [89]
C	(dC)	4.15	5.95	5.37	5.44	5.42	5.48 [90]
CoO	(RS)	0.00	4.53	–	4.01	3.62	2.5 [91]
GaN	(ZB)	1.88	3.68	3.10	3.30	3.26	3.29 [92]
ZnS	(ZB)	2.36	4.18	3.65	3.85	3.82	3.91 [85]
MnO	(RS)	1.12	3.87	2.55	3.66	3.60	3.9 [93]
WO_3	(M)	1.92	3.79	3.24	3.50	3.47	
BN	(ZB)	4.49	6.51	6.24	6.34	6.33	
HfO_2	(M)	4.32	6.65	6.38	6.68	6.68	
AlN	(WZ)	4.33	6.31	6.07	6.24	6.23	
ZnO	(WZ)	1.07	3.41	3.06	3.73	3.78	
Al_2O_3	(Cr)	6.31	8.84	9.42	9.65	9.71	
MgO	(RS)	4.80	7.25	7.97	8.24	8.33	
LiCl	(RS)	6.54	8.66	9.42	9.57	9.62	
NaCl	(RS)	5.18	7.26	8.55	8.73	8.84	
LiF	(RS)	9.21	12.28	15.48	15.83	16.15	
H_2O	(XI)	5.57	8.05	11.19	11.44	11.71	
Ar	(cF)	8.78	11.20	14.40	14.54	14.67	
Ne			15.20	23.32		23.67	
ME			−0.3	0.0		0.3	
MA			1.08	0.5		0.5	
MRE			10.8	−1.1		3.3	
MA			21.1	9.6		7.8	

*The … sed her … wo reported values 6.1 and 6.4 eV.

MAE	0.46	0.21	
MARE	5.9%	4.6%	

- **Similar accuracy as GW for energy gaps**

Energy Gaps

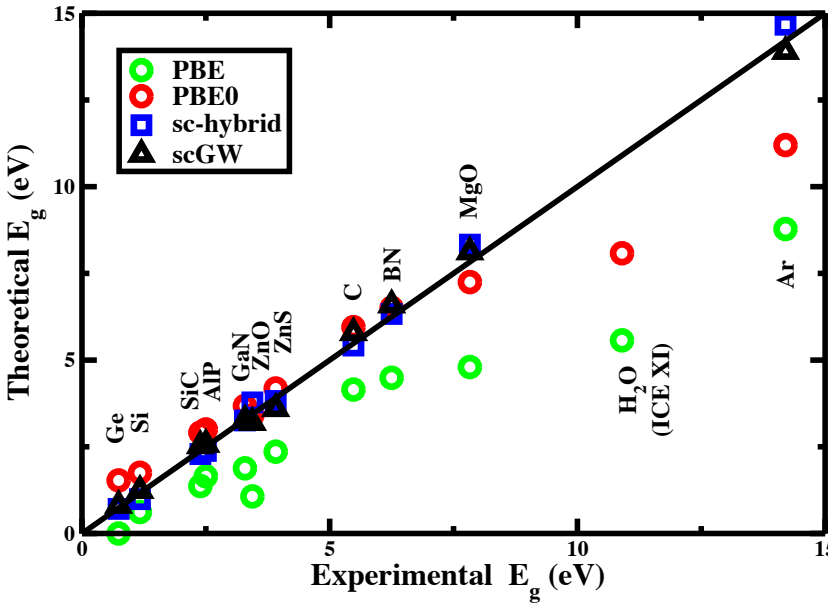

* Shishkin, et al. *PRB.* **75**, 235102 (2007). ** Shishkin, et al. *PRL.* **99**, 246403 (2007).

Comparison with experiment: electronic gaps

	Type	PBE $\alpha = 0$	PBE0 $\alpha = 0.25$	hybrid $\alpha = 1/\epsilon_\infty^{\mathrm{PBE}}$	hybrid $\alpha = 1/\epsilon_\infty^{\mathrm{PBE0}}$	sc-hybrid $\alpha = 1/\text{sc-}\epsilon_\infty$	Exp.
Ge	(dC)	0.00	1.53	–	0.77	0.71	0.74 [85]
Si	(dC)	0.62	1.75	0.96	1.03	0.99	1.17 [85]
AlP	(ZB)	1.64	2.98	2.31	2.41	2.37	2.51 [86]
SiC	(ZB)	1.37	2.91	2.23	2.33	2.29	2.39 [87]
TiO_2	(Ru)	1.81	3.92	2.83	3.18	3.05	3.3 [88]
NiO	(RS)	0.97	5.28	2.00	4.61	4.11	4.3 [89]
C	(dC)	4.15	5.95	5.37	5.44	5.42	5.48 [90]
CoO	(RS)	0.00	4.53	–	4.01	3.62	2.5 [91]
GaN	(ZB)	1.88	3.68	3.10	3.30	3.26	3.29 [92]
ZnS	(ZB)	2.36	4.18	3.65	3.85	3.82	3.91 [85]
MnO	(RS)	1.12	3.87	2.55	3.66	3.60	3.9 [93]
WO_3	(M)	1.92	3.79	3.24	3.50	3.47	3.38 [94]
BN	(ZB)	4.49	6.51	6.24	6.34	6.33	6.25 [95][a]
HfO_2	(M)	4.32	6.65	6.38	6.68	6.68	5.84 [96]
AlN	(WZ)	4.33	6.31	6.07	6.24	6.23	6.28 [97]
ZnO	(WZ)	1.07	3.41	3.06	3.73	3.78	3.44 [98]
Al_2O_3	(Cr)	6.31	8.84	9.42	9.65	9.71	8.8 [99]
MgO	(RS)	4.80	7.25	7.97	8.24	8.33	7.83 [100]
LiCl	(RS)	6.54	8.66	9.42	9.57	9.62	9.4 [101]
NaCl	(RS)	5.18	7.26	8.55	8.73	8.84	8.6 [102]
LiF	(RS)	9.21	12.28	15.48	15.83	16.15	14.2 [103]
H_2O	(XI)	5.57	8.05	11.19	11.44	11.71	10.9 [104]
Ar	(cF)	8.78	11.20	14.40	14.54	14.67	14.2 [105]
Ne	(cF)	11.65	15.20	23.32	22.99	23.67	21.7 [105]

Comparison with experiment: bandwidths

- Improved bandwidths
- Improved d band positions
- ZnO: still under-bound, similar to GW calculations

	PBE	PBE0	sc-hybrid	Exp.
	α = 0	α = 0.25	α = 1/sc-ε_∞	
Si	11.9	13.4	12.4	12.5
C	13.4	23.6	23.0	23.0
Ge	--	14.0	12.9	12.9
SiC	15.4	17.0	16.4	16.9
LiF	3.1	3.3	3.4	3.5
MgO	4.6	5.0	5.2	4.8
ZnO	6.1	7.0	7.2	9.0
TiO_2	5.7	6.4	6.1	~6.0

	PBE $\alpha=0$	PBE0 $\alpha=0.25$	sc-hybrid $\alpha=1/\text{sc-}\epsilon_\infty$	G_0W_0 * RPA	GW_0 * RPA	Exp.
GaN	-13.8	-15.7	-16.6	-16.0	-16.9	-17.0
ZnO	-5.0	-6.0	-6.3	-6.2	-6.6	-7.5,-8.81
ZnS	-6.3	-7.8	-7.5	-7.0	-7.5	-9.03

* Shishkin, et al. *PRB.* **75**, 235102 (2007).

Summary and Conclusions

- We used computational spectroscopy coupled to ab initio molecular dynamics to predict promising materials for solar energy conversion

- Several of our predictions were confirmed by experiment

- We interpreted several experiments on oxides

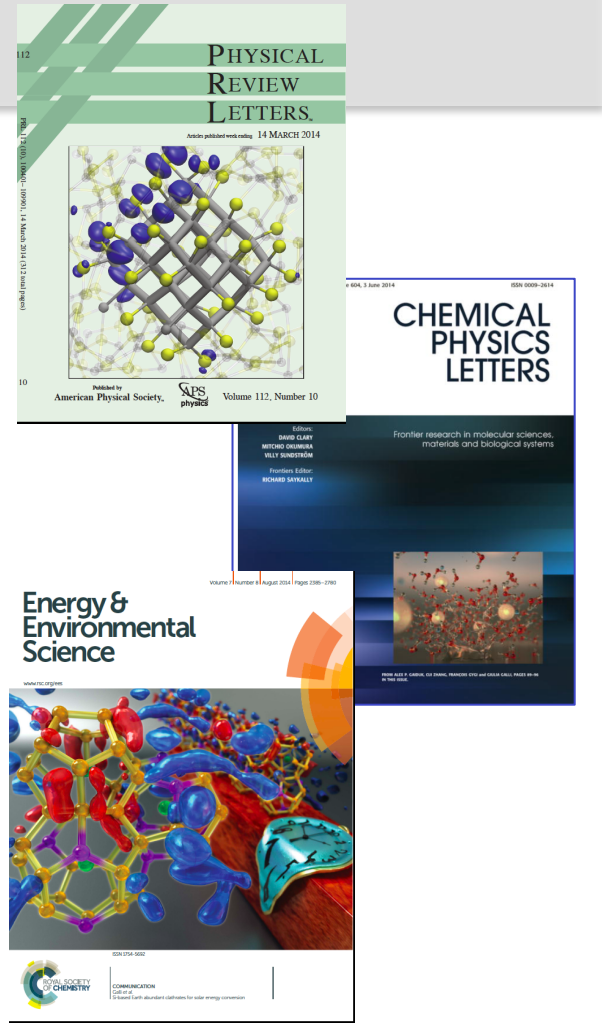

Complexity of materials & processes calls for the ability to compute multiple properties

Many Thanks To My Collaborators

http://galligroup.uchicago.edu/

THE INSTITUTE FOR MOLECULAR ENGINEERING

T.A. Pham (UCD), M. Govoni (U.Chicago), D. Lu (BNL), D.Rocca (U. Lorraine, France), H-V. Nguyen (Univ. Hanoi, Vietnam), Y. Ping (Caltech), H.Wilson (U.Melbourne, Australia)

M.Voros (UCD), N. Brawand (UCD), Yuping He (UCD), S.Wippermannn (Max Planck, Dusseldorf)

G. Zimanyi (UCD)
F. Gygi (UCD)
K-Y Choi (U. Wiscounsin)

S.Kauzlarich (UCD)
A.Gali (U.Budapest)

N.S.Lewis and H.B.Gray (Caltech)

Work funded by NSF, DOE, ARL ; Computer time: INCITE @ANL, LLNL, NERSC